Aerodynamic Heating to Corrugation Stiffened Structures in Thick Turbulent Boundary Layers

Harold J. Brandon* and Robert V. Masek†
McDonnell Douglas Astronautics Company—East, St. Louis, Mo.
and
James C. Dunavant‡
NASA Langley Research Center, Hampton. Va.

The results of an experimental program to evaluate heat transfer and pressure distributions on corrugation roughened flat plates in thick turbulent boundary layers are presented. The experimental program consisted of tests in the tunnel wall boundary layers of the Langley Unitary Plan Wind Tunnel (UPWT) and Continuous Flow Hypersonic Tunnel (CFHT) at freestream Mach numbers of 2.5, 3.5, 4.5, and 10.3. Tests in the UPWT were conducted at a freestream Reynolds number/m of 10.8 x 10^6 and in the CFHT, at Reynolds numbers/m of 1.3 to 5.8 x 10^6. The test configurations consisted of 50.8 cm x 50.8 cm panels with corrugated beads of two different peak amplitudes, 0.61 cm and 0.29 cm. The angle of the corrugated beads relative to the flow direction was varied between 0° (aligned) and 90° (normal). The measured peak and average heat transfer are analyzed and correlated in terms of the bulk boundary layer, internal boundary layer, and geometric parameters. The data are also compared with similar data for thinner boundary layers, and with previously published correlation techniques.

Nomenclature

a = speed of sound
C_f = skin friction coefficient
C_p = specific heat
h = heat transfer coefficient, $q/(T_{aw}-T_w)$
k_e = equivalent sand grain roughness height
L = wave length in direction of flow
M = Mach number
N_{St} = Stanton number, $h/\rho_\infty U_\infty C_p$
P = static pressure
q = heat transfer rate
Re = Reynolds number
S = surface distance from top of wave
T = temperature
U = velocity
α = local wave surface angle
γ = ratio of specific heats, $\gamma = 1.4$
ϵ = maximum wave amplitude from wave midline
δ = boundary-layer thickness
δ^* = boundary-layer displacement thickness
δ_s = laminar sublayer thickness
θ = momentum thickness
$\bar{\theta}$ = temperature ratio $(T_{T_\epsilon}-T_w)/(T_{T_\infty}-T_w)$
μ = molecular viscosity
ϕ = angle of corrugations relative to freestream flow direction
ρ = density

Subscripts

av = average
aw = adiabatic wall
FP = flat plate
ke = based on equivalent sand grain roughness height
max = maximum
T = total, surface distance of one wave
w = wall
ϵ = wave height
∞ = freestream

Presented as Paper 75-190 at the AIAA 13th Aerospace Sciences Meeting, Pasadena, California, January 20-22, 1975; submitted January 28, 1975; revision received May 15, 1975. This study was performed at McDonnell Douglas Astronautics Company-East under Contract NAS1-12901. The authors wish to thank H. B. Wilson of NASA-MSFC for sponsoring many of the tests conducted for this study, and R. B. Dirling of MDAC-West for the predicted average heat transfer coefficient calculations.

Index categories: Boundary Layers and Convective Heat Transfer—Turbulent; Supersonic and Hypersonic Flow.

*Technical Specialist, Thermodynamics.
†Manager, Thermodynamics (Acting). Member AIAA.
‡Aerospace Engineer. Member AIAA.

Introduction

STRUCTURAL stiffening of outer surface panels of aerodynamic vehicles by means of surface corrugations is an attractive means of reducing surface weight and surface deflections under load. A number of studies, including some early space shuttle designs, have included such surfaces on hypersonic lifting vehicles where the corrugations, in addition to providing stiffening, tolerate the thermal expansions of the metal caused by aerodynamic heating. The surface waves interact with the local flow and cause drastic deviations of local heating from that expected for laminar and turbulent smooth wall analyses; changes are expected both in heating distribution and in average heating. Alignment of the wave with local streamwise flow directions so that their effect can be ignored does not appear to be a feasible solution for most hypersonic vehicles where thick boundary layers produce large amounts of crossflow.

The effect of surface corrugations and surface irregularities on boundary layers has received much attention in the last 10 years. [1-5] Most of the results obtained in these investigations are summarized by Bertram.[6] Bertram's work, although quite extensive, did not include data for which the boundary layer was orders of magnitude thicker than the surface corrugation height. This is an important practical problem because very thick turbulent boundary layers are often encountered under certain flight conditions. The present study is concerned with heat transfer when the corrugations are deeply submerged in a thick turbulent boundary layer.

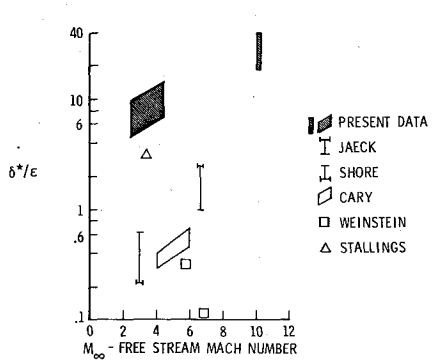

Fig. 1 Comparison of turbulent heating data.

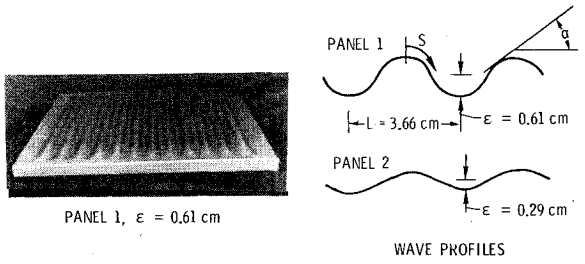

Fig. 2 Surface corrugations and photograph of 51×51 cm test panel.

The flow conditions for which heating distributions have been measured on corrugated surfaces and wavy walls in turbulent boundary layers are shown in Fig. 1, which gives the ratio of the displacement thickness to the roughness height vs the local edge Mach number for an equivalent smooth surface. The present data are seen to greatly extend the range of data available on corrugated surfaces in turbulent boundary layers. These data were obtained by testing full-scale corrugation roughened panels in the wall boundary layer of a supersonic and hypersonic wind tunnel.

In this paper, the experimental program used to obtain the data is described. The data are analyzed and correlated in terms of the pertinent flow and geometric parameters. The present data and correlations are compared with the available thin boundary-layer data and with previously published correlation techniques

Model and Instrumentation

Two corrugation roughened flat panels were tested in this study. Both plates were 50.8 x 50.8 x 2.54 cm and were fabricated from nominally 0.043-cm-thick 321 stainless steel. The more deeply corrugated panel had a peak amplitude of 0.61 cm above and below the wave mean line and the shallow corrugated panel, 0.29 cm. The two panels were identical in shape except for the wave amplitude. A photograph of one of the panels and profiles of the two wave shapes are shown in Fig. 2. Each panel contained 12½ corrugations (wave cycles), which ran the entire length of the model. Each wave profile was essentially constant over an 18.8-cm section in the center, and tapered to zero at 1.91 cm from the panel edge. With the corrugations aligned parallel with the flow (configuration termed $\phi=0°$), the corrugations were composed of parabolic segments. With the corrugations aligned normal to the flow (termed $\phi=90°$), the corrugations were constructed of circular arcs connected by straight line segments. For both plates, the wavelength was equal to 3.66 cm.

Both corrugated models were instrumented with thermocouples and pressure orifices. With the waves normal to the flow direction, the 2nd, 6th, and 10th waves were instrumented with thermocouples along the model centerline in the direction of the flow. In the same fashion, the pressure taps were located on the 2nd and 10th waves slightly off the centerline.

A smooth flat plate (50.8 x 50.8 x 2.54 cm) was also fabricated from 321 stainless steel (0.127 cm thick). This model was instrumented with thermocouples only. Flat plate heating data were measured so that the heating data obtained on the corrugation roughened panels could be referenced to local measured flat plate values.

Test Program

The two corrugated panels and the flat plate were tested in the turbulent wall boundary layer of the Langley Unitary Plan Wind Tunnel (UPWT) and the Continuous Flow Hypersonic Tunnel (CFHT). The panels were attached to an adapter plate, which was mounted flush with the wind-tunnel wall. For the UPWT tests, the adapter plate contained a mechanical actuator assembly so that the corrugation orientation angle relative to the freestream direction could be varied from 0° to 90°. For the CFHT tests, the corrugations could only be tested at 0°, 15°, 75°, and 90° due to the arrangement of the injection mechanism.

The flow and geometric conditions for the present study are listed in Table 1. The flat plate was also tested at the six different Mach number and Reynolds number combinations. The boundary-layer parameters displacement thickness, and momentum thickness listed for the CFHT were calculated from measured pitot and total temperature profiles through the boundary layer by assuming a constant freestream static pressure through the boundary layer. For the UPWT, δ^* and θ were obtained by calculating the boundary-layer development on the wind-tunnel wall using the numerical method described by Keller and Cebeci.[7] This method has been extended to compressible flows by Cebeci, and this latter computer program was used for the present calculations. Good agreement was obtained in a comparison of the velocity profiles predicted by this method and the experimental velocity profiles measured by Couch.[8] Beckwith's correlation[9] was used to calculate the laminar sublayer thickness for the CFHT. This correlation, however, did not contain data in the range of interest for the UPWT test conditions. Therefore, for the UPWT conditions, δ_s was calculated from the following equation,[10]

$$\delta_s = 11\ \mu_w a_w / \gamma P_{FP} M_\infty (C_f/2)^{1/2}$$

where C_f was taken from the boundary-layer solution. Values

Table 1 Test conditions

M_∞	Re_∞/m	ϕ, deg	ϵ, cm	$T_w/T_{T\infty}$	δ^*, cm	θ, cm	δ_s, cm	$h_{FP}{}^a W/(m^2 K)$
2.5	10.8×10^6	0,30,90	0.29	0.81	2.87	0.83	0.010	62.5
		0,7.5,15	0.61					
		30,60,90						
3.5		0,30,90	0.29		3.63	0.64	0.020	32.8
		0,7.5,15						
		30,60,90	0.61					
4.5		0,30,90	0.29		4.34	0.48	0.037	15.7
		0,7.5,15	0.61					
		30,60,90						
10.3	1.3×10^6	0,15,75,90	0.29	0.30	11.63	0.82	0.813	1.14
			0.61					
	3.3×10^6		0.29		11.56	0.83	0.447	2.20
			0.61					
	5.8×10^6		0.29		11.25	0.73	0.351	3.22
			0.61					

[a]Value at center of test panel.

calculated in this manner were superimposed on Beckwith's correlation. Fairly good agreement was found between these calculations and an extrapolation of the Beckwith correlation.

Experimental Results

External flow and geometric conditions (Table 1) were varied so that the effects of Mach number, Reynolds number, flow angle, and wave height on heat transfer distribution could be determined. The heating data to the corrugated surfaces have been normalized to values of local heating measured on a flat plate at the same test condition. Tests of the flat plate revealed heat transfer gradients in the vertical direction in both the UPWT and CFHT. The gradients were more severe in the CFHT and are due to the manner in which the boundary layer develops in the nozzle. Heating to the flat plate was lowest at the center of the test panel and increased toward the upper and lower edges. By normalizing the corrugated panel data to the local undisturbed heating rate, the effects of heat transfer gradients in the vertical direction were eliminated. Axial gradients in the heat transfer distributions over the model length were negligible for both facilities.

Heating distributions that display typical trends of the results with the test variables are shown in Figs. 3 - 7. In several instances, major differences were found between the present results and those for thin boundary layers. In previous results, peak heating and pressure on multiple waves decreased with increasing wave cycle, however, similar decreases did not occur for the present data. The absence of any decay in peak heating is clearly seen in Fig. 3, which presents heating distributions over the 2nd, 6th, and 10th waves. Thus, for a given set of flow conditions, the heating distribution is independent of wave cycle. This result suggests that surface rouighness deeply submerged in the boundary layer has only a small effect on the external flow. Pitot pressure profiles taken through the boundary layer at the end of the corrugations were almost identical to the smooth wall profiles, indicating that the external flow is unaffected by, or adjusts rapidly to, any disturbance produced by individual waves. On the other hand, wave cycles located in thin boundary layers drastically affect the external flow conditions,[4,6] which results in significant decreases in heating and pressure for successive waves.

Heat transfer distributions for the sixth wave measured in hypersonic flow ($M_\infty = 10.3$, $\mathrm{Re}/m = 3.3 \times 10^6$) are presented for flow angles of 0°, 15°, 75°, and 90° in Fig. 4. As for previous thin boundary-layer results, the highest peak heating occurs for flow normal to the corrugations ($\phi = 90°$) and is not much less when the flow is inclined to the corrugations by as little as 15°. Oil flows indicated that these distributions are the result of flow separation in the valley and subsequent reattachment on the forward surface of the following wave. Such a flow model is compatible with most of the measured heating distributions; however, exceptions were noted at $M_\infty = 3.5$ and 4.5 where the distributions on the 6th wave were frequently similar to that shown in the valleys ($S/S_{\mathrm{TOTAL}} \approx 0.5$) in Fig. 5. Oil flow tests were not made for these conditions and no adequate explanation for this anomaly is known; however, it is suspected that it may be caused by a secondary separation and reattachment within the larger separated region.

The heating also varies from valley to crest when the flow is aligned with the corrugations ($\phi = 0°$). This results from boundary-layer growth at the upstream end of the panel as the valleys and crests taper out to a flat plate (see photograph of Fig. 2).

During the supersonic tests, the Mach number was varied from 2.5 to 4.5 while the Reynolds number was held constant at $\mathrm{Re}/m = 10.8 \times 10^6$. In the hypersonic tests, the Reynolds number was varied from 1.3×10^6 to 5.8×10^6 per meter at a constant Mach number of 10.3. Increasing both of these variables substantially increases the peak heat transfer as shown in Figs. 5 and 6. It should be noted that the trend of increasing heating with Reynolds number differs from the thin

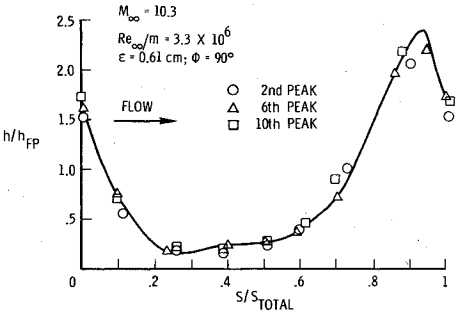

Fig. 3 Effect of wave cycle on heating distribution.

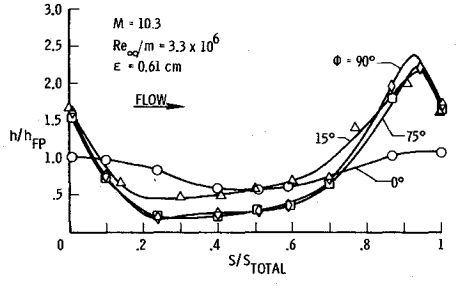

Fig. 4 Effect of flow angle on heating distribution.

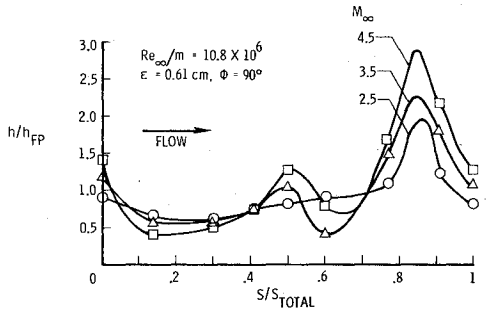

Fig. 5 Effect of Mach number on heating distribution.

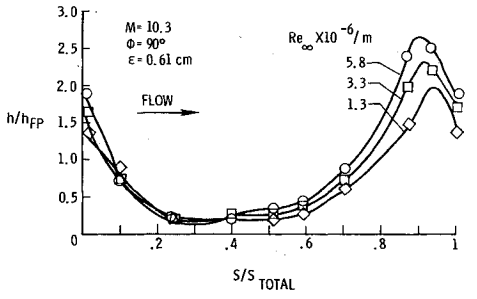

Fig. 6 Effect of Reynolds number on heating distribution.

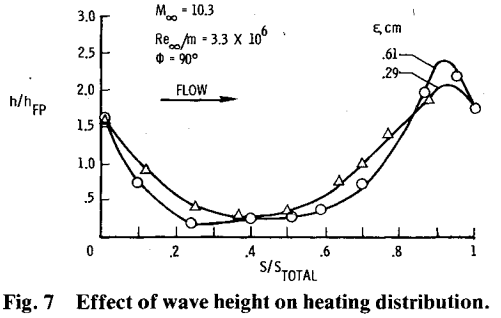

Fig. 7 Effect of wave height on heating distribution.

boundary-layer data of Cary,[4] which shows the peak heating is inversely proportional to Reynolds number.

In the present tests, the variation in corrugation height (amplitude) yielded results that are radically different from those for thin boundary layers. Heat transfer and pressure were found to be relatively insensitive to wave amplitude for all flow conditions investigated. The effect of wave height shown in Fig. 7 is much less than that of either Mach number or Reynolds number. This result may be of great importance in sizing of corrugations of heat shields for vehicle applications where the boundary layers are thick. For example, the data of Cary for thin boundary layers, obtained for approximately the same freestream conditions and geometric parameters as for the present supersonic tests, indicate that increasing the wave height by a factor of two would increase the heating nearly threefold. This result shows that caution must be exercised in extrapolating either thick or thin boundary-layer data to conditions where the wave height to boundary-layer thickness is substantially different from the test conditions.

Analysis

Theoretical Flow Model

Oil flow patterns obtained during the tests indicated flow separation just aft of the wave peak and reattachment on the following wave. A flow model (Fig. 8) consistent with the oil flow patterns was postulated in hope that the heating distribution on a complete wave could be predicted. In this model, flow separation is assumed to occur near the top of the wave and an upstream and downstream attached boundary layer are assumed to initiate at the reattachment point (which is approximated by the location of the measured peak pressure). Edge stagnation conditions for the two new boundary layers are assumed to be those at the reattachment point. These stagnation conditions are used in conjunction with the measured surface pressures to define local edge conditions, which are used as input to a nonsimilar compressible turbulent boundary-layer solution. Further details of the flow model are given by Brandon.[11]

The surface pressure distribution utilized as input to the boundary-layer calculations for the flow model is shown in Fig. 9 for a supersonic case ($M_\infty = 4.5$, $\mathrm{Re}_\infty/m = 10.8 \times 10^6$) with the flow normal to the waves. The pressure distributions for $M_\infty = 2.5$ and 3.5 are also shown for comparison to demonstrate the relatively insignificant effect of Mach number on the pressure distribution. The surface pressure along the wave is essentially equal to the flat plate pressure except at the reattachment point. Prediction of the heating distribution using the flow model for this case is shown in Fig. 10. The theory follows the trend of data, but the predicted values are higher than the measured values. Similar results were found for the other supersonic cases. It was found that the predicted heating distribution was primarily a function of the total temperature at the reattachment point. Certainly, more analysis is needed to improve and assess the range of validity of the flow model.

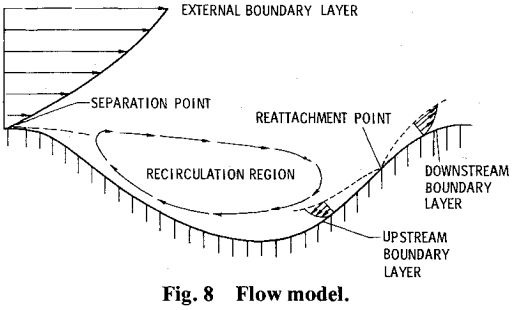

Fig. 8 Flow model.

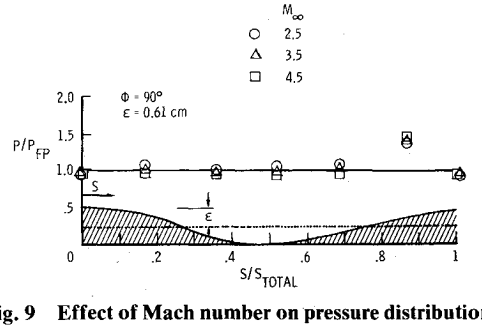

Fig. 9 Effect of Mach number on pressure distribution.

Data Correlation

A previous study of turbulent reattachment heating for thin boundary layers by Kim and Parkinson[12] showed that the heating and pressure throughout the reattachment region correlated with the expression $h/h_{FP} = (P/P_{FP}).8$. This expression offers a technique for computing heat flux distributions directly from pressure distributions, and was subsequently used by Nestler.[13] Holden[14] reported a similar correlation for the maximum turbulent reattachment heat flux, but with an exponent of 0.85 instead of 0.8.

The variation in the heating rate with the local pressure for the present study is shown in Fig. 11. This correlation reveals two separate relationships. In the separated region ($P \approx P_{FP}$), the heating is independent of pressure. In the attached flow regime, the heating ratio is approximately proportional to the square of the pressure ratio rather than the eight-tenths power, which more nearly represents the reattachment heating for thin turbulent boundary layers. Therefore, for roughness deeply submerged in a turbulent boundary layer, the increase over flat plate heating is much greater than the corresponding increase over flat plate pressure.

As discussed in Ref. 11, correlation studies showed that the following internal boundary-layer temperature parameter evaluated at the peak amplitude proved useful in correlating the data:

$$\bar{\theta} = (T_{T_\epsilon} - T_w)/(T_{T_\infty} - T_w)$$

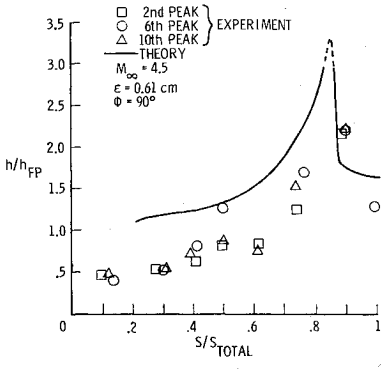

Fig. 10. Comparison of experimental and theoretical heating distribution.

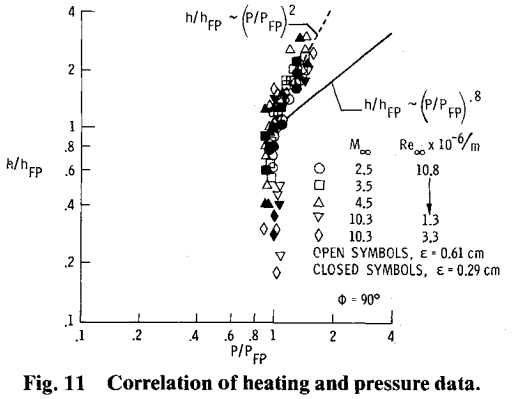

Fig. 11 Correlation of heating and pressure data.

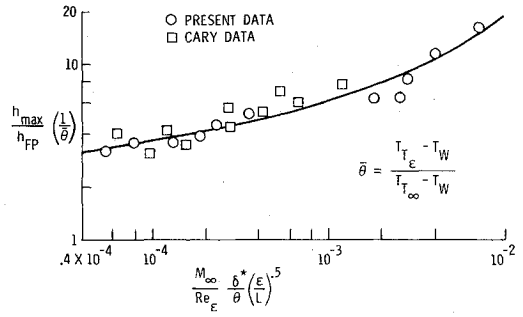

Fig. 12 Correlation of maximum heating with bulk parameters.

The first attempt of correlating the data in terms of the temperature parameter is shown in Fig. 12. The maximum heating data divided by $\bar{\theta}$ for the flow normal to the waves are directly proportional to the Mach number, shape factor, and the square root of the wave amplitude/wave length and inversely proportional to the Reynolds number based on the wave amplitude. Some of the Cary data[4] shown in Fig. 12 also agree with this correlation. (The $\bar{\theta}$ used for Cary's data was 1.) However, comparison of this correlating form with the present data for other flow angles showed that different forms of the governing parameters would be needed.

The maximum heating measured during this study are summarized in Table 2. These maximum values were obtained from faired curves through the data. An automated multiple regression analysis (MRA) designed to fit multiple variables was employed to obtain consistent, nonbiased correlations of these data. (The $M_\infty = 10.3$, $Re_\infty/m = 5.8 \times 10^6$ data were not available at the time the MRA was made; however, these data are compared to the resulting prediction.) The MRA computer program is described in detail in Ref. 15.

Table 2 Maximum wave heating

$Re_{,\infty}/m$	M_∞	ϕ, deg	$\epsilon = 0.29$ cm h_{max}/h_{FP}	$\epsilon = 0.61$ cm h_{max}/h_{FP}
10.8×10^6	2.5	0	1.03	0.9
	3.5		0.98	0.95
	4.5		1.0	1.20
	2.5	7.5	[a]	1.4
	3.5		[a]	1.5
	4.5		[a]	2.1
	2.5	15	[a]	1.5
	3.5		[a]	1.7
	4.5		[a]	2.4
	2.5	30	1.6	1.7
	3.5		1.8	1.9
	4.5		2.5	2.5
	2.5	60	[a]	1.9
	3.5		[a]	2.1
	4.5		[a]	2.7
	2.5	90	1.9	2.0
	3.5		2.2	2.3
	4.5		2.85	2.9
1.3×10^6	10.3	0	0.95	1.01
		15	1.53	1.7
		75	1.55	1.85
		90	1.75	2.0
3.3×10^6		0	1.03	1.06
		15	1.7	2.3
		75	1.9	2.3
		90	2.1	2.4
5.8×10^6		0	0.98	1.03
		15	1.7	2.50
		75	2.30	2.50
		90	2.25	2.65

[a] No data taken.

During the course of the correlation activity, it was discovered that another important geometric parameter was the sine of the local surface angle at reattachment. It was found that by including sin α as a variable, the temperature parameter $\bar{\theta}$ could be eliminated from the list of variables. Several good fits to all the present data using $\bar{\theta}$ or sin α were obtained, and are presented in Ref. 16. However, comparison of the correlations with data sets for thinner boundary layers showed that only one of the correlations was in reasonable agreement with the other data. (Excellent agreement between the present correlations and the other data sets was not expected due to the differences in the trends of the thick and thin boundary-layer data.) This correlation is presented in Fig. 13. All the present data (except for $\phi = 0°$) and data for thinner boundary layers are presented in this figure. The angle ϕ enters in the correlation through the wave length by the relation $\cos(90° - \phi) = L_{90°}/L$ where $L_{90°} = 3.66$ cm. Although there is considerable scatter, the data for thin boundary layers do tend to group around this correlation. In order for this correlation to be applied, the angle α must be known. However, the geometry of the separated flow was not determined in this study, and still needs to be investigated. Therefore, for design studies, either the correlation involving $\bar{\theta}$ in Ref. 16 should be used, or the correlation in Fig. 13 should be approximated by setting the angle α equal to the maximum surface angle α_{max}.

Bertram[6] found that Jaeck's correlation[3] gave a fair-to-good estimate of the maximum heating trends for thin turbulent boundary layers. Jaeck's correlation is compared with the present data obtained in thick turbulent boundary layers for various Mach numbers in Fig. 14 as a function of the flow angle ϕ. Jaeck's correlation greatly underpredicts the data for thick boundary layers for all flow conditions and all flow angles. Also shown in this figure is the correlation of Fig. 13 which closely represents the data. Similar disagreement between the present data and Jaeck's correlation was noted for the hypersonic Mach number data for all Reynolds numbers. Based on these results, it appears Jaeck's correlation is not valid for corrugation roughened surfaces deeply submerged in thick boundary layers where flow separation occurs. As

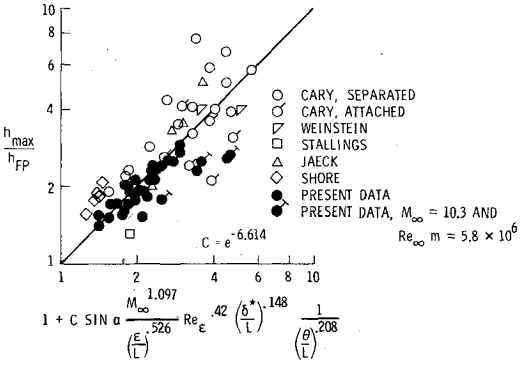

Fig. 13 Correlation of maximum heating.

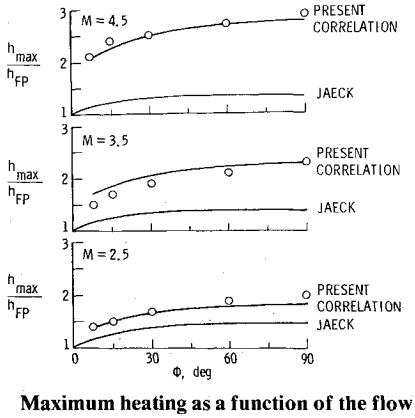

Fig. 14 Maximum heating as a function of the flow angle.

discussed by Cary,[4] Jaeck's theory gave a good estimate for thin boundary layers except when the boundary layer was separated prior to the wave. Where there was extensive separation, the theory seriously underestimated the maximum heating, as in the present case.

Average heat transfer to rough surfaces for re-entry conditions has received much attention in the past few years. As a result, several correlations for rough surface average heat transfer have been proposed. A simple approximate turbulent heating formulation developed by Powars[17] was believed to be one of the more reliable approaches.

Average heat transfer values from the present experiments are compared with the Powars correlation in Fig. 15. The equivalent sand grain roughness, k_e, used in this correlation was calculated using Dirling's analysis.[18] It is seen that the data fall well below the Powars equation for $10k_e/\delta_s > 10$. Following Powars and letting

$$10k_e/\delta_s = \mathrm{Re}_{ke}(N_{\mathrm{St,\,FP}})^{1/2}$$

the present average heating data are represented by the equation

$$N_{\mathrm{St,\,av}}/N_{\mathrm{St,\,FP}} = 1 + A[\log_{10}(\mathrm{Re}_{ke}(N_{\mathrm{St,\,FP}})^{1/2}) - 1]$$

where $A = 1/6$ rather than 2/3 as recommended by Powars.

The surprising disagreement with the Powars correlation led to a further analysis of the average heating data using the recent method proposed by Dirling. It was found that for the flow normal to the shallow waves, the average heating could be predicted within a few percent using Dirling's method. However, it was also found that the deep wave data could only be predicted if the equivalent sand grain roughness height was based on the wave half-height. Using this half-height, the average heating could also be predicted within a few percent. The reason for this phenomenon is not completely understood and needs more investigation. A summary comparison of the present average heating data and the Dirling theory is shown in Table 3.

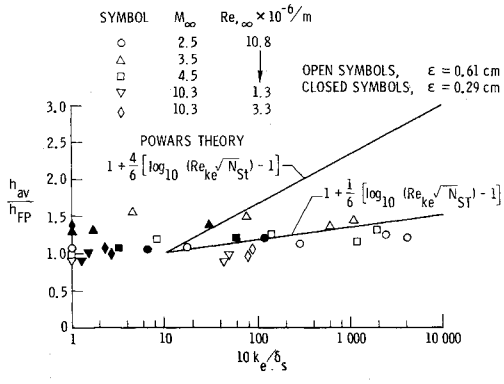

Fig. 15 Average heating compared with Powars correlation.

Table 3 Comparison of average heating with Dirling's prediction

M_∞	Re_∞/m	ϵ(cm)	ϕ, deg	MEAS h_{av}/h_{FP}	PRED h_{av}/h_{FP}
2.5	10.8×10^6	0.29	90°	1.20	1.29
2.5		0.61		1.20	1.48
3.5		0.29		1.20	1.23
3.5		0.61		1.31	1.38
4.5		0.29		1.36	1.14
4.5		0.61		1.44	1.37
10.3	1.3×10^6	0.29		0.98	1.00
	1.3×10^6	0.61		0.96	0.93
	3.3×10^6	0.29		1.03	1.00
	3.3×10^6	0.61		1.04	1.04

Summary of Results

An extensive set of tests has been conducted for the heating and pressure distributions on corrugation roughened surfaces in thick supersonic and hypersonic turbulent boundary layers. The data and analysis yielded the following results:

1) Large increases in heating were measured for all corrugation angles greater than 0°. As with thin boundary layers, the largest changes occurred for small sweep angles.

2) Significant effects of Mach number and Reynolds number were detected. The present peak heating data indicated a direct proportionality to Reynolds number, whereas the thin boundary-layer data were inversely proportional to Reynolds number.

3) In contrast to the data for thin boundary layers, the heating distributions for the flow normal to the waves were found to be essentially independent of wave amplitude/wave length and wave cycle.

4) The local heating was found to be proportional to the square of the pressure, rather than the eight-tenths power which approximates the thin boundary-layer reattachment relation. For the present data, changes in pressure were much less than the corresponding changes in heating due to the corrugations.

5) A flow model was postulated to predict the wave heating distribution. For a supersonic case ($M_\infty = 4.5$), the flow model followed the trend of the data, but the predicted values were higher than the measured values.

6) Based on a total temperature in the undisturbed boundary layer at the wave height, the maximum heat transfer data for the flow normal to the waves were directly proportional to the Mach number, shape factor, and the square root of the wave amplitude/wave length, and inversely proportional to the Reynolds number based on the wave amplitude.

7) For all flow orientation angles, the peak heating data were correlated in terms of bulk boundary layer, internal boundary layer, and geometric parameters. Data for thin boundary layers were found to group around one of the correlations developed from the present thick boundary-layer data.

8) Jaeck's correlation greatly underpredicted the maximum heating data for all flow conditions and all flow angles.

9) Average heating values were found to fall well below the Powars correlation.

10) Dirling's method was found to predict the average heating within a few percent for the smaller amplitude wave. Also, by using an equivalent sand grain roughness based on the wave half-height, this method also matched the average heating values for the larger amplitude wave.

References

[1] Shore, C. P., Dixon, S. C., and Griffith, G. E., "Experimental Pressures and Turbulent Heat Transfer Coefficients Associated With Sinusoidal Protuberances on a Flat Plate at a Mach Number of 3," NASA TN D-1626, March 1963.

[2] Stallings, R. L., Jr. and Collins, L. K., "Heat Transfer Measurements on a Flat Plate and Attached Protuberances in a Turbulent Boundary Layer at Mach Numbers of 2.65, 3.51, and 4.44," NASA TN D-2428, Sept. 1964.

[3] Jaeck, C. L., "Analysis of Pressure and Heat Transfer Tests on Surface Roughness Elements With Laminar and Turbulent Boundary Layers," NASA CR-537, 1966.

[4] Cary, A. M., Jr. and Morrisette, E. L., "Effect of Two-Dimensional Multiple Sine-Wave Protrusions on the Pressure and Heat Transfer Distributions for a Flat Plate at Mach 6," NASA TN D-4437, March 1968.

[5] Weinstein, L. M., "Effects of Two-Dimensional Sinusoidal Waves on Heat Transfer and Pressure Over a Flat Plate at Mach 8," NASA TN D-5937, Aug. 1970.

[6] Bertram, M. H., Weinstein, L. M., Cary, A. M., Jr. and Arrington, J. P., "Heat Transfer to a Wavy Wall in Hypersonic Flow," *AIAA Journal*, Vol. 5, No. 10, Oct. 1967, pp. 1760-1767.

[7]Keller, H. B. and Cebeci, T., "Accurate Numerical Methods for Boundary-Layer Flows," AIAA Paper 71-164, Washington, D.C. 1971.

[8]Couch, L. M., "Flow Field Measurements Downstream of Two Protuberances on a Flat Plate Submerged in a Turbulent Boundary Layer at Mach 2.49 and 4.44," NASA TN D-5297, July 1969.

[9]Beckwith, I. E., Harvey, W. D., and Clark, F. L., "Comparison of Turbulent Boundary-Layer Measurements at Mach Number 19.5 with Theory and an Assessment of Probe Errors," NASA TN D-6192, June 1971.

[10]Reda, D. C., "Compressible Turbulent Skin Friction on Rough and Rough/Wavy Walls in Adiabatic Flow," NOLTR 74-34, Feb. 1974, Naval Ordnance Lab., White Oak, Silver Spring, Md.

[11]Brandon, H. J., Masek, R. V., and Dunavant, J. C., "Aerodynamic Heating to Corrugation Stiffened Structures in Thick Turbulent Boundary Layers," AIAA Paper 75-190, Pasadena, Calif., 1975.

[12]Kim, B. S. C. and Parkinson, T. W., "Flap Turbulent Heating Characteristics Obtained From a Hypersonic Shock Tunnel," AIAA Paper 71-598, Palo Alto, Calif. 1971.

[13]Nestler, D. E., "An Engineering Analysis of Reattaching Shear Layer Heat Transfer," AIAA Paper. 72-717, Boston, Mass. 1972.

[14]Holden, M. S., "Shock-Wave Turbulent Boundary-Layer Interaction in Hypersonic Flow," AIAA Paper 72-74, Washington, D.C., 1972.

[15]Christensen, H. E. and Kipp, H. W., "Data Correlation and Analysis of Arc Tunnel and Wind-Tunnel Tests of RSI Joints and Gaps," MDC Rept. E1033, McDonnell Douglas Corp., Los Angeles, Calif.; also NASA CR-134346, Jan. 1974.

[16]Brandon, H. J. and Masek, R. V., "Measurement and Correlation of Aerodynamic Heating to Surface Corrugation Stiffened Structures in Thick Turbulent Boundary Layers," NASA CR-132503, Sept. 1974.

[17]Powars, C. A., "Surface Roughness Effects on Reentry Heating," TM 71-10, July 1971, Aerotherm Corp., Mountain View, Calif.

[18]Dirling, R. B., Jr., "A Method for Computing Roughwall Heat Transfer Rates on Re-entry Nosetips," AIAA Paper 73-763, Palm Springs, Calif., 1973.